



A high-performance $\text{Bi}_2\text{O}_3/\text{Bi}_2\text{SiO}_5$ p-n heterojunction photocatalyst induced by phase transition of Bi_2O_3



Haojie Lu^{a,1}, Qiang Hao^{a,b,1}, Tong Chen^a, Linghua Zhang^a, Daimei Chen^{a,*}, Chao Ma^b, Wenqing Yao^{b,*}, Yongfa Zhu^{b,*}

^a Beijing Key Laboratory of Materials Utilization of Nonmetallic Minerals and Solid Wastes, National Laboratory of Mineral Materials, School of Materials Science and Technology, China University of Geosciences, Beijing 100083, China

^b Department of Chemistry, Tsinghua University, Beijing 100084, China

ARTICLE INFO

Keywords:
 $\text{Bi}_2\text{O}_3/\text{Bi}_2\text{SiO}_5$ heterojunction
 Photocatalysts
 $\beta\text{-Bi}_2\text{O}_3$

ABSTRACT

In this work, $\text{Bi}_2\text{O}_3/\text{Bi}_2\text{SiO}_5$ p-n heterojunction photocatalyst was successfully fabricated via a facile one-step synthesis using $\text{Bi}(\text{NO}_3)_3$ and nano- SiO_2 as precursors. With the increasing amount of SiO_2 , $\alpha\text{-Bi}_2\text{O}_3$ gradually transferred into $\beta\text{-Bi}_2\text{O}_3$, and $\text{Bi}_2\text{O}_3/\text{Bi}_2\text{SiO}_5$ p-n heterojunction was obtained at the same time. The as-prepared samples were systematically characterized by XRD, scanning electron microscopy (SEM), energy-dispersive spectrometry (EDS), transmission electron microscopy (TEM), X-ray photoelectron spectroscopy (XPS), UV-vis diffuse reflectance spectroscopy (DRS). The $\text{Bi}_2\text{O}_3/\text{Bi}_2\text{SiO}_5$ heterojunction photocatalysts exhibited higher photocatalytic activity than $\alpha\text{-Bi}_2\text{O}_3$ on the degradation of organic pollutants under simulated sunlight irradiation. The enhanced photocatalytic activity could be ascribed to the larger specific surface area, the larger contact angle, the formation of $\beta\text{-Bi}_2\text{O}_3$ and construction of p-n heterojunction. More importantly, the phase transition mechanism of Bi_2O_3 in $\text{Bi}_2\text{O}_3/\text{Bi}_2\text{SiO}_5$ heterojunction photocatalyst was proposed, which is significant for the theoretical study and application of photocatalytic materials.

1. Introduction

Nowadays, with the rapid development of industry, the freshwater resources are facing more and more severe problems, which enable to lead to environmental pollution and cause serious threat to human beings [1–3]. Recent years, semiconductor photocatalytic technology, with its advantages of energy saving and environmental friendliness, has attracted great interests of scientists and it has broad application prospect in sewage disposal [4–6]. Nevertheless, there are several drawbacks of single-component photocatalysts, such as poor visible light utilization, rapid recombination of photo-generated electrons and holes pairs, which limits the application of photocatalytic materials [7–9].

Various methods have been proposed to enhance photocatalytic activity, such as morphology control, elements doping or noble metal deposition [10–14]. Construction of heterojunction semiconductors has been proved to be an effective method to overcome the shortcomings of single-component photocatalysts. For example, Ju et al. [15] reported that the calcined $\text{Bi}_2\text{WO}_6/\text{BiVO}_4$ heterojunction enhanced its photocatalytic activity, which could be attributed to the effective separation

of the photoinduced electron-hole pairs at the heterojunction interface, the widened light absorption range and the better crystallinity. Chen et al. [16] also synthesized AgI/BiVO_4 heterojunction with high-efficiency degradation of tetracycline under visible light irradiation. In binary semiconductors, the energy gap between the two semiconductors allows photo-generated carriers to be injected from the energy level of one type of semiconductor particle into the energy level of another, resulting in efficient and long-term charge separation. Undoubtedly, heterojunction photocatalysts system is a significant strategy for the improvement of photocatalytic activity.

Bismuth silicate (Bi_2SiO_5) is a newly discovered compound in the Aurivillius family, first reported in 1996 [17,18]. It is recognized that Bi_2SiO_5 is alternately stacked in a two-dimensional structure by $(\text{Bi}_2\text{O}_2)^{2+}$ and $(\text{SiO}_3)^{2-}$ layer [19,20]. It has been applied to the field of photocatalysis and has lots of advantages, such as non-toxicity, chemical stability and excellent photocatalytic activity [21–23]. However, Bi_2SiO_5 can only be applied in the ultraviolet region because of its wide bandgap (~ 3.5 eV) [24,25]. Therefore, it is necessary to take effective methods to expand the photo-response range of Bi_2SiO_5 .

Bismuth oxide (Bi_2O_3), also as a member of bismuth-based

* Corresponding authors.

E-mail addresses: chendaimei@cugb.edu.cn (D. Chen), yaowq@tsinghua.edu.cn (W. Yao), zhuyf@tsinghua.edu.cn (Y. Zhu).

¹ These authors contributed the same to this manuscript.

semiconductors, has α , β , γ and δ , four kinds of crystalline form, corresponding to monoclinic crystalline form, tetragonal crystalline form, body-centered cubic crystalline form and face-centered cubic crystalline form, respectively [26,27]. Thereinto, α -Bi₂O₃ and β -Bi₂O₃ could be candidates for Visible light catalysis. α -Bi₂O₃ is stable and has a bandgap of 2.8 eV which indicates that it can respond to visible light. However, α -Bi₂O₃ fabricated by calcination and the like tends to agglomerate, which leads to its lower photocatalytic activity. The band gap of β -Bi₂O₃ is about 2.3 eV and its light absorption property is much stronger than that of α -Bi₂O₃. Howbeit, β -Bi₂O₃ belongs to the metastable state and is unstable at normal temperature. Thus the practical application of single-component α -Bi₂O₃ or β -Bi₂O₃ to photocatalysis has been greatly limited. Nevertheless, the bandgap structure of α -Bi₂O₃, β -Bi₂O₃ and Bi₂SiO₅ are well aligned so that the construction of Bi₂O₃/Bi₂SiO₅ heterojunction enables to accelerate the migration and separation rate of photo-generated carriers and improve the photocatalytic activity. Zhang et al. [28] reported the solar photocatalytic results of Bi₂O₃/Bi₂SiO₅ formed in mesoporous SiO₂ microspheres. Although this method has improved the photocatalytic activity to a certain degree, the synthesis of this method was too complicated, consuming too much energy and leading to environmental pollution. Hence it is difficult to be applied in mass production.

In this work, Bi₂O₃/Bi₂SiO₅ heterojunction photocatalysts were prepared by a facile one-step calcination method. The photocatalytic activity of Bi₂O₃/Bi₂SiO₅ heterojunction photocatalysts was much higher than α -Bi₂O₃ because of the larger specific surface area, larger contact angle, the formation of β -Bi₂O₃ and construction of p-n heterojunction. Meanwhile, the raw materials are easy to obtain, and the synthesis is facile, energy saving and environmental friendly. Therefore, the Bi₂O₃/Bi₂SiO₅ heterojunction photocatalysts prepared in this paper is beneficial to industrial mass production and application. More importantly, the phase transition mechanism of Bi₂O₃ in Bi₂O₃/Bi₂SiO₅ heterojunction photocatalyst was proposed, which is significant for the theoretical study and application of photocatalytic materials.

2. Experimental section

2.1. Material preparation

All chemicals used were reagent grade and used without further purification. Bi(NO₃)₃·5H₂O was dried at 60 °C for 2 h to obtain Bi(NO₃)₃ powder without crystal water. After that, the Bi(NO₃)₃ powder was transferred to a quartz agate mortar and then nano-SiO₂ powder was added to the Bi(NO₃)₃ powder. The two powders were well mixed and ground for 15 min and the mixture was transferred to a corundum crucible. It was heated to 600 °C within 2.5 h and kept at that temperature for 4 h. The obtained powder was Bi₂O₃/Bi₂SiO₅ heterojunction photocatalysts. The products in which the mass fraction of SiO₂ is 1%, 5%, 10%, 15% and 20% were named as BiSi-1, BiSi-2, BiSi-3, BiSi-4 and BiSi-5, respectively. The preparation method of the samples was showed in Chart 1. α -Bi₂O₃ was obtained by the same way and condition without adding SiO₂.

2.2. Characterization

A series of characterization tests were carried out to study morphology and structure of samples and the mechanism of photocatalytic activity enhancement. The instruments and details of XRD, SEM, TEM, XPS, DRS, BET, and electrochemical characterization in this article are the same as those used in our previous work [29]. The OCA15pro Contact angle analyzer (German Dataphysics) was used to perform water contact angle measurement. The electron paramagnetic resonance (EPR) was carried out with a Bruker ESR 300E, using dimethyl pyridine N-oxide as the radical scavenger.

2.3. Photocatalytic activity test

The photocatalytic activity of the samples was evaluated by the degradation of methylene blue (MB), phenol (PhOH) and 2,4-dichlorophenol (2, 4-DCP) under simulated solar light irradiation which was provided by a 500 W xenon lamp without using cutoffs and the average light intensity is 35 mW/cm². Photocatalyst sample (100 mg) was uniformly dispersed in an aqueous solution of MB (50 ml, 10 ppm), PhOH (50 ml, 10 ppm) or 2, 4-DCP (50 ml, 10 ppm). Before light irradiation, the suspensions were magnetically stirred in the dark for 30 min to get the absorption-desorption equilibrium. Afterward, the lamp was turned on and 3 mL aliquots were sampled at certain time intervals and filtered. The concentration of MB was analyzed by measuring the maximum absorption wavelength (664 nm) using a Hitachi U-3900 UV-vis spectrophotometer. The concentration of PhOH and 2, 4-DCP was measured by high-performance liquid chromatography (HPLC) (Shimadzu LC-20AT).

3. Results and discussion

3.1. Structure and morphology

X-ray diffraction (XRD) was used to characterize the crystal structure, crystallinity and composition of α -Bi₂O₃ and Bi₂O₃/Bi₂SiO₅ heterojunction photocatalysts. The XRD patterns of the α -Bi₂O₃, Bi₂O₃/Bi₂SiO₅ heterojunction photocatalysts were shown in Fig. 1. The three strongest diffraction peaks with 2θ at 27.39°, 33.24° and 46.34° in Fig. 1a corresponded to the (-121), (-202) and (041) planes of α -Bi₂O₃ (JCPDS: 71-0465), respectively. α -Bi₂O₃ belongs to the monoclinic system ($a = 0.58496$ nm, $b = 0.81648$ nm, $c = 0.75101$ nm) P21/c space group. In the XRD patterns of BiSi-1, BiSi-2 and BiSi-3 heterojunction photocatalysts (Fig. 1a), three strong diffraction peaks with 2θ at 27.39°, 33.24° and 46.34° corresponded to the (-121), (-202) and (041) planes of α -Bi₂O₃, while the three strong diffraction peaks with 2θ at 11.62°, 23.89° and 29.23° correspond to the (200), (310) and (311) planes of Bi₂SiO₅ (JCPDS: 36-0287), respectively. Bi₂SiO₅ belongs to the orthorhombic system ($a = 1.5217$ nm, $b = 0.5477$ nm, $c = 0.5325$ nm) Cmc21 space group. In the XRD patterns of BiSi-1, BiSi-4 and BiSi-5 heterojunction photocatalysts, three strong diffraction peaks with 2θ at 11.62°, 23.89° and 29.23° corresponded to the (200), (310) and (311) planes of Bi₂SiO₅, while the diffraction peaks with 2θ of 27.93° and 32.70° correspond to the (201) and (220) planes of β -Bi₂O₃ (JCPDS: 77-5341), respectively. β -Bi₂O₃ belongs to the monoclinic system ($a = 0.77400$ nm, $b = 0.77400$ nm, $c = 0.56446$ nm) P21/c space group. The XRD results showed that the samples BiSi-1 and BiSi-2 were mainly composed of α -Bi₂O₃ and Bi₂SiO₅, while the samples BiSi-4 and BiSi-5 were mainly composed of β -Bi₂O₃ and Bi₂SiO₅, and most specifically, BiSi-3 was composed of α -Bi₂O₃, β -Bi₂O₃ and Bi₂SiO₅.

FTIR analysis was carried out to investigate the chemical states of the synthesized α -Bi₂O₃ and Bi₂O₃/Bi₂SiO₅ heterojunctions. In Fig. S1, no peak was detected in α -Bi₂O₃, whereas three absorption peaks at 866, 952 and 1029 cm⁻¹ were observed in Bi₂O₃/Bi₂SiO₅ heterojunctions. The absorption band at about 864 cm⁻¹ matched the stretching vibration of the Bi-O-Si bond [30]. The peaks near 952 cm⁻¹ corresponded to the stretching vibrations of the [SiO₃]²⁻ tetrahedral [31]. The peaks near 1032 cm⁻¹ were generated by the stretching vibrations of the Si-O bond [30]. These peaks were well matched with Bi₂SiO₅, indicating that Bi₂SiO₅ was formed after the addition of SiO₂.

The morphology and size of Bi₂O₃/Bi₂SiO₅ heterojunction photocatalysts were first examined by SEM. It can be seen clearly from Fig. 2a that the α -Bi₂O₃ had a bulk structure, leading to a reduction of photocatalytic effect. As shown in Fig. 2b–e, after the addition of nano-SiO₂, not only Bi₂SiO₅ formed, but also the aggregation of α -Bi₂O₃ was significantly inhibited. All the Bi₂O₃/Bi₂SiO₅ heterojunction photocatalysts were scattered, which made them smaller in size and larger in the specific surface area compared with α -Bi₂O₃. The elements



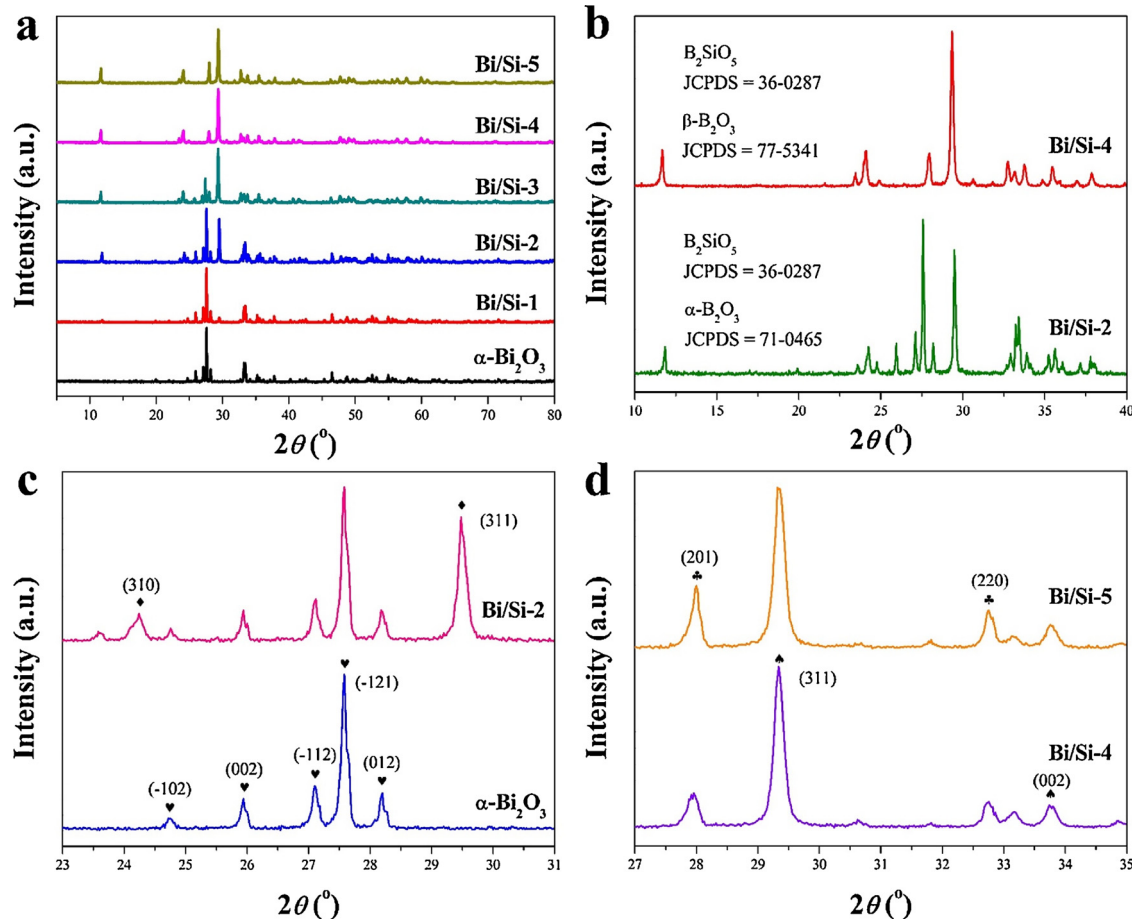
Chart 1. A flow diagram of the sample preparation method.

distribution of the sample was carried out by Energy Dispersive Spectrometer (EDS) mapping. The results showed that there were three kinds of elements Bi, Si, O, and three kinds of elements distributed evenly in $\text{Bi}_2\text{O}_3/\text{Bi}_2\text{SiO}_5$ heterojunction photocatalysts, which further illustrated the sample was uniform.

The detailed microstructure of the $\text{Bi}_2\text{O}_3/\text{Bi}_2\text{SiO}_5$ heterojunction was further studied by TEM and HRTEM. As can be seen from Fig. 3a, the size of $\alpha\text{-Bi}_2\text{O}_3$ was bulk structure and relatively larger, about 2 μm . The spacing between the layered lattice diffraction fringes of 0.331 nm and the (−112) plane of the $\alpha\text{-Bi}_2\text{O}_3$ were well matched. Fig. 3c showed some sheets of sample BiSi-4 having a microscopic size of about

30 nm. Fig. 3d showed the lattice diffraction fringes produced by the BiSi-4 with a lattice spacing of 0.381 and 0.256 nm coincided well with the (511) plane of Bi_2SiO_5 and (102) plane of $\beta\text{-Bi}_2\text{O}_3$, respectively.

XPS has been widely employed to study the surface chemical composition and state of materials [32,33]. Fig. 4a was the survey spectrum of the $\alpha\text{-Bi}_2\text{O}_3$ and BiSi-4. It was evident that Bi, Si and O elements were detected in sample BiSi-4, whereas Si element was not detected in sample $\alpha\text{-Bi}_2\text{O}_3$. As shown in Fig. 4b, the two strongest peaks at 158.7 and 163.9 eV were assigned to the orbital $4f_{7/2}$ and $4f_{5/2}$ of Bi^{3+} in $\alpha\text{-Bi}_2\text{O}_3$, respectively. Moreover, the binding energy of the orbital $4f_{7/2}$ and $4f_{5/2}$ of Bi^{3+} in BiSi-4 increased by 0.4 eV compared with $\alpha\text{-Bi}_2\text{O}_3$,

Fig. 1. (a) XRD patterns of $\alpha\text{-Bi}_2\text{O}_3$ and $\text{Bi}_2\text{O}_3/\text{Bi}_2\text{SiO}_5$ heterojunctions.

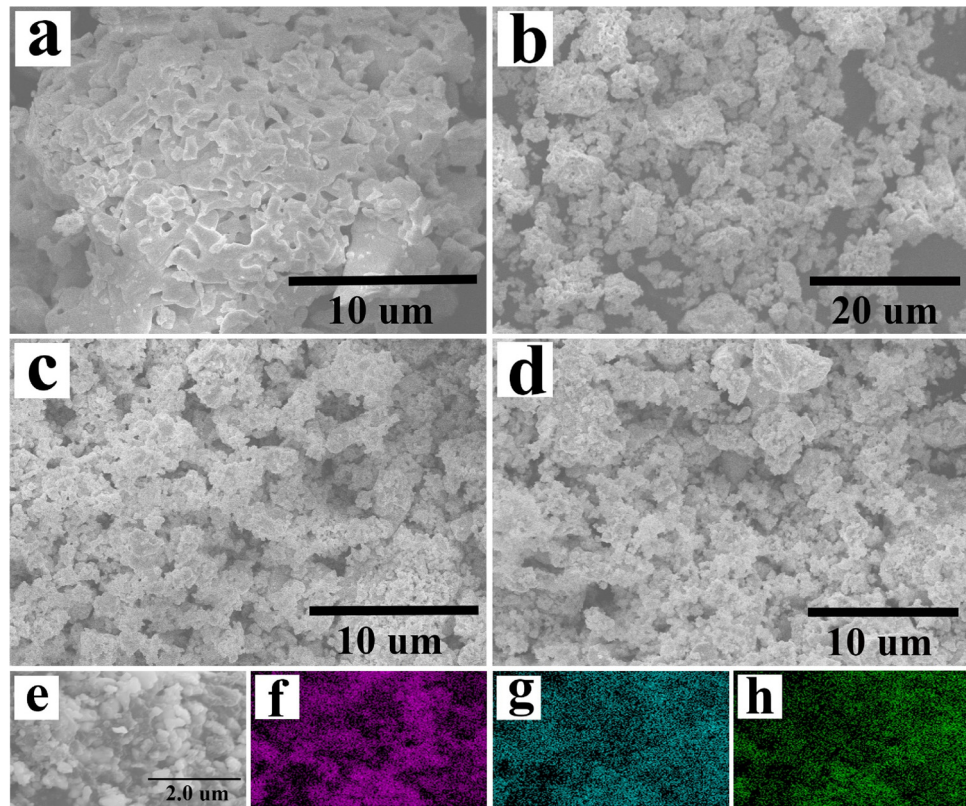


Fig. 2. SEM images of the as-prepared samples: α - Bi_2O_3 (a), BiSi-1 (b), BiSi-2 (c), BiSi-3 (d), BiSi-4 (e); EDS elemental distributions for Bi, Si and O of BiSi-4 (f), (g) and (h).

indicating that the chemical states of Bi surroundings had changed, which possibly owing to the strong interaction between β - Bi_2O_3 and Bi_2SiO_5 [33]. Fig. 4c was the narrow spectrum of Si 2p in sample BiSi-4, from which corresponded to SiO_5^{6-} at 103.1 eV. In Fig. 4d, the curve was fitted by two O 1s orbits of the sample, and two peaks with different binding energies could be obtained by the peak splitting. In Fig. 4d, the O 1s peak of α - Bi_2O_3 at 529.7 and 531.6 eV were associated

with the O^{2-} in α - Bi_2O_3 [34]. In the O 1s spectrum of BiSi-4, the peak at 530 eV was attributed to Bi-O in Bi_2SiO_5 and β - Bi_2O_3 [35,36]. The strong peak at 532.4 eV which moved up 0.8 eV in comparison with that of α - Bi_2O_3 is the characteristic peak of O_2 on the surface of Bi_2SiO_5 [37]. BiSi-4 is smaller in size and larger in the specific surface area than α - Bi_2O_3 , which allows a large amount of O_2 to adsorb to the surface of Bi_2SiO_5 . The increase of specific surface area facilitates the adsorption

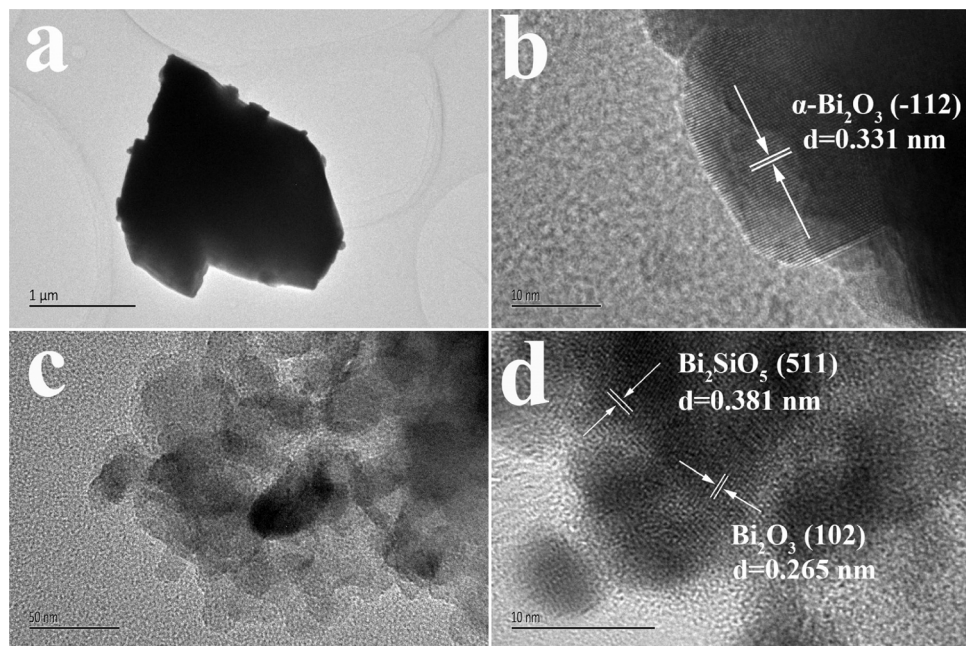


Fig. 3. TEM and HRTEM images of sample α - Bi_2O_3 (a, b) and BiSi-4 (c, d).

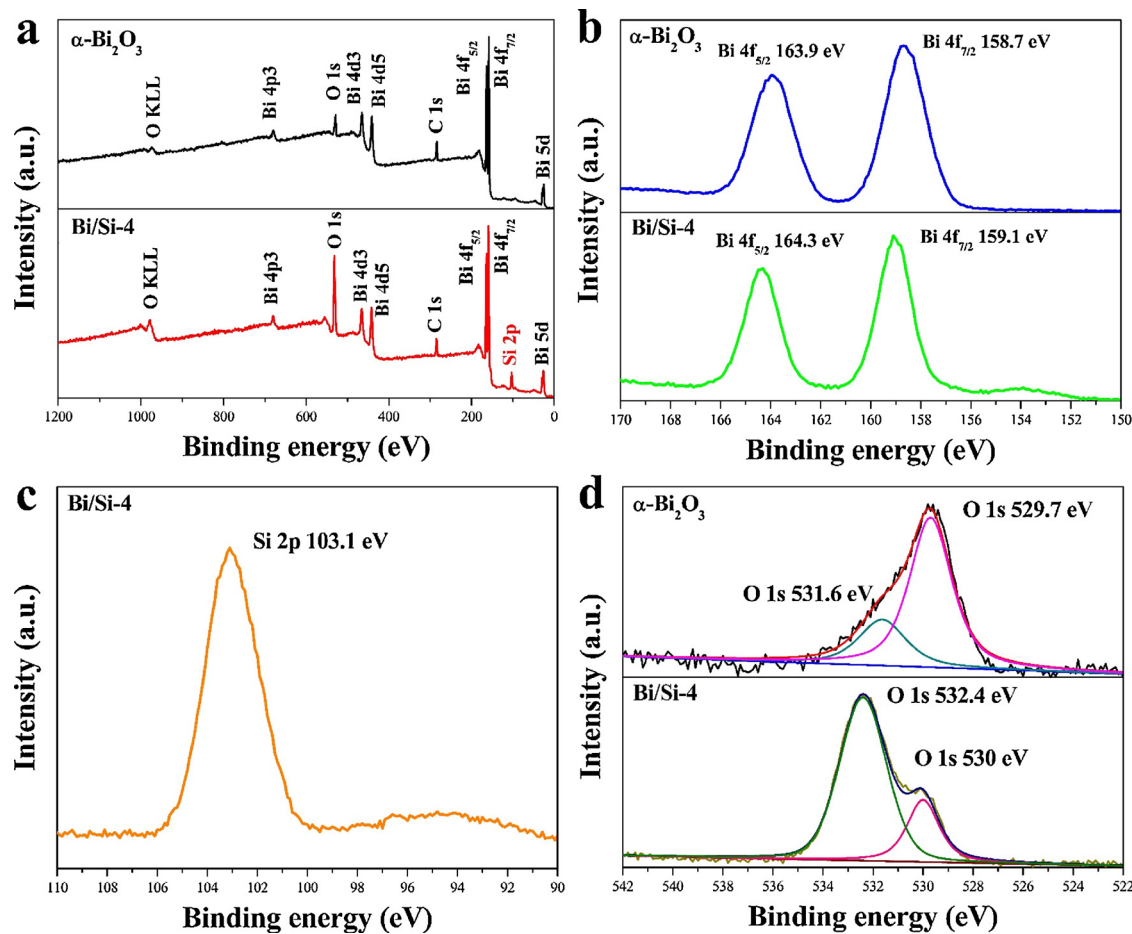


Fig. 4. XPS spectrum of α - Bi_2O_3 and BiSi-4: the XPS survey spectrum (a), Bi 4f (b), Si 2p (c) and O 1s (d).

of large amounts of O_2 on the surface of BiSi-4, which is conducive to the generation of $\text{O}_2^{\cdot-}$ with strong oxidation, thereby enhancing the photocatalytic activity of BiSi-4.

3.2. Photocatalytic activity

The photocatalytic activity of the samples was evaluated by photocatalytic degradation of organic pollutant MB, 2,4-DCP and PhOH with α - Bi_2O_3 and $\text{Bi}_2\text{O}_3/\text{Bi}_2\text{SiO}_5$ heterojunction photocatalysts under simulated sunlight irradiation. Fig. 5a and b showed the k values for MB degradation by α - Bi_2O_3 and $\text{Bi}_2\text{O}_3/\text{Bi}_2\text{SiO}_5$ heterojunction photocatalysts. As can be obtained from Fig. 5a, the k value increases gradually from BiSi-1 to BiSi-4, which indicated that the degradation activity increases gradually with the increasing amount of SiO_2 content in the reactants. It was obvious that the sample BiSi-4 had the highest photocatalytic efficiency and it was three times higher than that of α - Bi_2O_3 . Fig. 5c–f are the chromatographic outflow curves of 2, 4-DCP and PhOH during the photodegradation process over α - Bi_2O_3 and BiSi-4, which shows that the peak area of the curves decreases gradually with the increase of time, and the removal efficiency of BiSi-4 was much higher than that of α - Bi_2O_3 . Fig. 5b–f indicated that the degradation activity of BiSi-4 was higher than α - Bi_2O_3 .

3.3. Photocatalytic mechanism

The absorption edge of the sample was determined by UV-vis diffuse reflectance spectra (DRS), and the bandgap of the samples was calculated by Kubelka-Munk formula [18,38,39]. According to Fig. 6, the absorption edge of α - Bi_2O_3 was 455 nm, and the bandgap was 2.75 eV, which mean that α - Bi_2O_3 enable to absorb visible light. The

content of Bi_2SiO_5 in the BiSi-1 sample was not high, so sample BiSi-1 had almost the same absorption edge wavelength and bandgap as α - Bi_2O_3 . When it came to BiSi-2, there were two obvious absorption edges, one of which was about 455 nm, the other was about 360 nm and the corresponding bandgap was 2.75 and 3.54 eV, respectively. These two absorption edges corresponded to two substances, α - Bi_2O_3 and Bi_2SiO_5 , respectively, indicating that α - Bi_2O_3 and Bi_2SiO_5 are present in $\text{Bi}_2\text{O}_3/\text{Bi}_2\text{SiO}_5$ heterojunction photocatalyst. For sample BiSi-3, there were three distinct absorption edges, namely, 360, 455 and 578 nm, corresponding to the bandgap of 3.54, 2.75 and 2.17 eV, respectively. This was because that there are three substances in the BiSi-3 sample, Bi_2SiO_5 , α - Bi_2O_3 and β - Bi_2O_3 . BiSi-4 and BiSi-5 have two absorption edges, with absorption edge wavelengths of 360 and 578 nm, corresponding to the bandgap of 3.54 and 2.17 eV, respectively, which belong to two kinds of substances existing in the sample, Bi_2SiO_5 and β - Bi_2O_3 .

Brunner-Emmet-Teller (BET) tests were carried out to study the specific surface area of α - Bi_2O_3 and BiSi-4. Fig. 7 showed the adsorption-desorption isotherms and specific surface area (illustration) of α - Bi_2O_3 and BiSi-4. The inset Fig. was the data of the specific surface area of the two samples. The results showed that the specific surface areas of α - Bi_2O_3 and BiSi-4 were $0.19013 \text{ m}^2 \text{ g}^{-1}$ and $6.54245 \text{ m}^2 \text{ g}^{-1}$, respectively. The A_{BET} of BiSi-4 was about 34.4 times as large as that of α - Bi_2O_3 , which was beneficial for the photocatalytic reaction.

Fig. 8 showed the contact angles of the α - Bi_2O_3 and BiSi-4. The contact angle of α - Bi_2O_3 in Fig. 8a was 107.9° , indicating that the surface of α - Bi_2O_3 was hydrophobic. Fig. 8b showed that the contact angle of BiSi-4 was 58.6° , indicating that the surface was hydrophilic. Namely, the liquid was more likely to wet the BiSi-4. The smaller the contact angle was, the better the hydrophilicity the sample had. Bi_2SiO_5

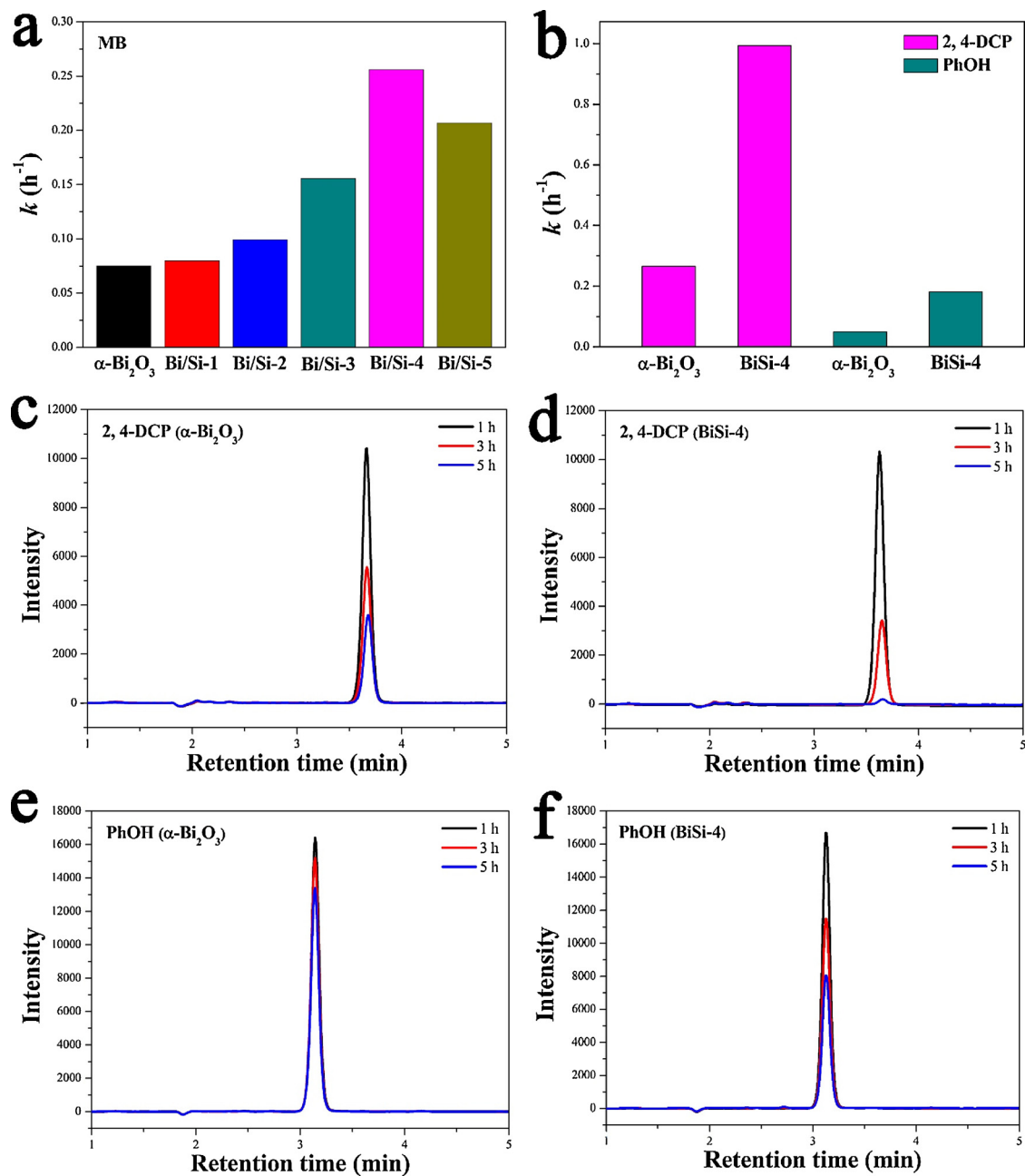


Fig. 5. The comparison of the apparent rate constants of α -Bi₂O₃ and Bi₂O₃/Bi₂SiO₅ heterojunctions for the degradation of MB (a), 2, 4-DCP and PhOH (b); chromatographic outflow curves of 2, 4-DCP during the photodegradation process over α -Bi₂O₃ (c) and BiSi-4 (d); chromatographic outflow curves of PhOH during the photodegradation process over α -Bi₂O₃ (e) and BiSi-4 (f).

was introduced so that the Bi₂O₃/Bi₂SiO₅ heterojunction is more hydrophilic relative to α -Bi₂O₃, which facilitated the contact of photocatalysts with contaminants in water to achieve better degradation.

EPR was also performed to confirm the reactive species in the degradation process. In Fig. S2, neither the O₂^{·-} signal nor the ·OH signal was detected of α -Bi₂O₃ both in dark and under sunlight irradiation. This result indicated that neither O₂^{·-} nor ·OH was the main reactive species in the process of degradation by α -Bi₂O₃. According to previous work, the main active species of α -Bi₂O₃ is hole [29]. In Fig. S2c, the BiSi-4 produced six signals, which was attributed to the presence of O₂^{·-} in light, while no signal was observed in the dark. In addition, no ·OH signal of BiSi-4 was detected in dark conditions or under sunlight irradiation (Fig. S2d). Compared with α -Bi₂O₃, Bi₂O₃/Bi₂SiO₅ heterojunction introduced much more O₂^{·-} in the photocatalytic process and thus improved photocatalytic degradation efficiency.

The photocurrent response of the catalysts showed a stable and fast anodic photocurrent response under repeated illumination (cycle 30 s). It can be seen from Fig. 9 that the relationship between the regular of their photocurrent and the constant rate k in the photodegradation is consistent. This mean that the construction of heterojunction made the transfer and separation speed of photogenerated charge carriers at the interface between α -Bi₂O₃ and Bi₂SiO₅ much higher.

In summary, four reasons for the enhancement of photocatalytic activity are given: (1) Bi₂O₃/Bi₂SiO₅ heterojunction photocatalysts have larger specific surface area than α -Bi₂O₃. This not only increased the separation efficiency of the electron-hole pairs but also increased the reaction contact area between the photocatalyst and the pollutants in the solution, thereby increasing the photocatalytic degradation efficiency. (2) The contact angles of Bi₂O₃/Bi₂SiO₅ heterojunction photocatalysts are larger than α -Bi₂O₃. The hydrophilicity of the

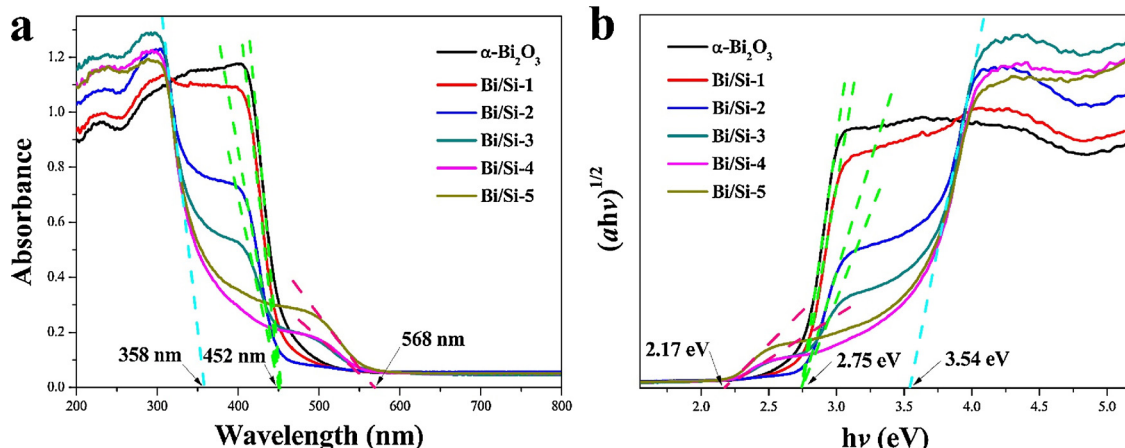


Fig. 6. (a) UV-vis diffuse reflectance spectra of α -Bi₂O₃ and Bi₂O₃/Bi₂SiO₅ heterojunctions; (b) the plot of $(ah\nu)^{1/2}$ vs $h\nu$ of the samples.

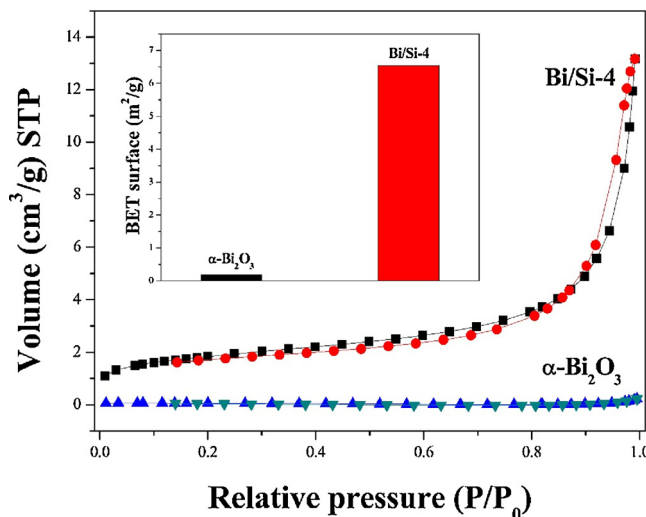


Fig. 7. N₂ adsorption-desorption isotherm of α -Bi₂O₃ and BiSi-4, the insert is the Specific surface area of α -Bi₂O₃ and BiSi-4.

heterojunction is significantly strengthened, which allows the photocatalyst to sufficient contact with the organic pollutants in aqueous solution, allowing the organic contaminants to be rapidly degraded. (3) The addition of nano-SiO₂ in the reactants results in not only the formation of Bi₂SiO₅ but also the formation the β -Bi₂O₃ in the product. β -Bi₂O₃ has a large visible light response range, improving the solar energy utilization. (4) The construction of p-n heterojunction. Bi₂SiO₅ is a typical n-type semiconductor (Fig. S3) and β -Bi₂O₃ is p-type [40,41]. So that they can form a p-n heterojunction, as a result, the separation of

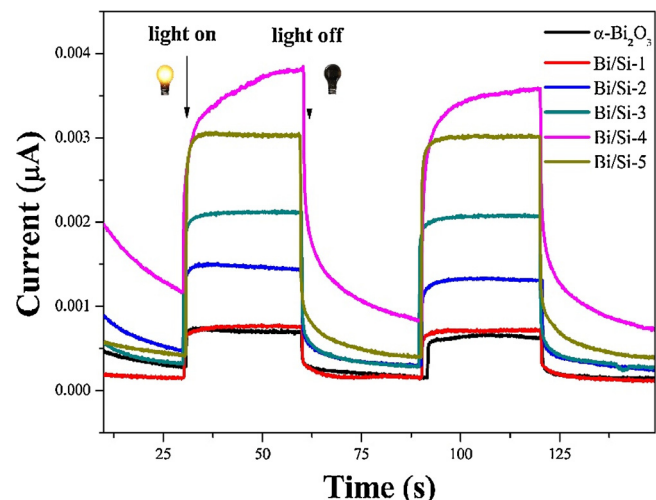


Fig. 9. Photocurrent responses of α -Bi₂O₃ and Bi₂O₃/Bi₂SiO₅ heterojunctions in Na₂SO₄ (0.1 M) aqueous solution.

electron-hole pairs was more effective and the recombination of electron-hole pairs was slowed down, thereby enhancing the photocatalytic efficiency. The results of the ESR test show that the photo-generated electrons react with the oxygen in the solution to form O₂^{·-}, which is the main reactive species for the catalytic degradation of organic pollutants.

In this work, the phase transition mechanism of Bi₂O₃ in Bi₂O₃/Bi₂SiO₅ heterojunction photocatalyst was proposed as follow. When SiO₂ was added into the raw materials and calcined at high

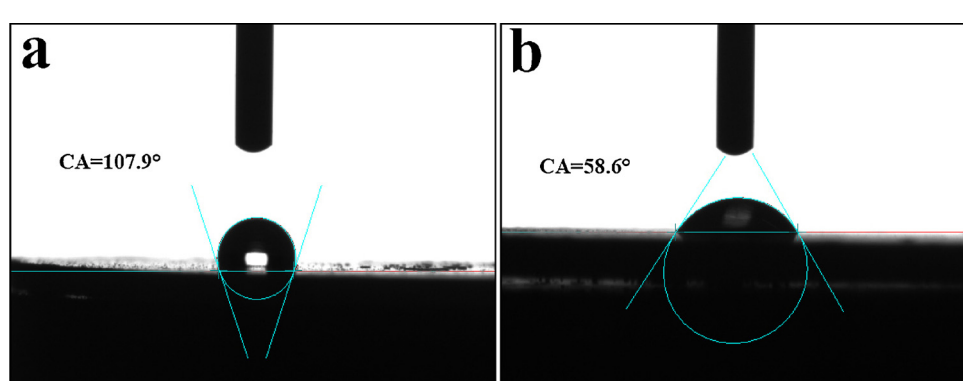
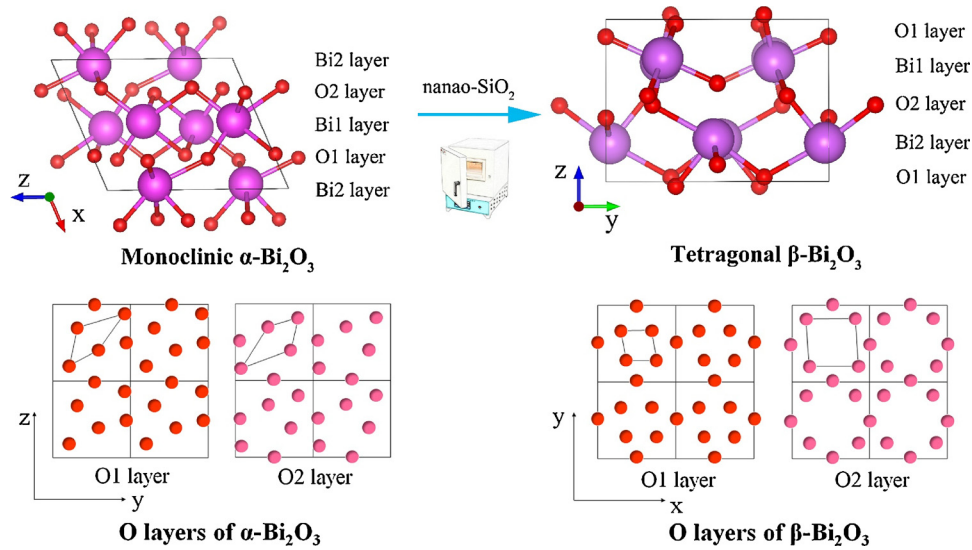
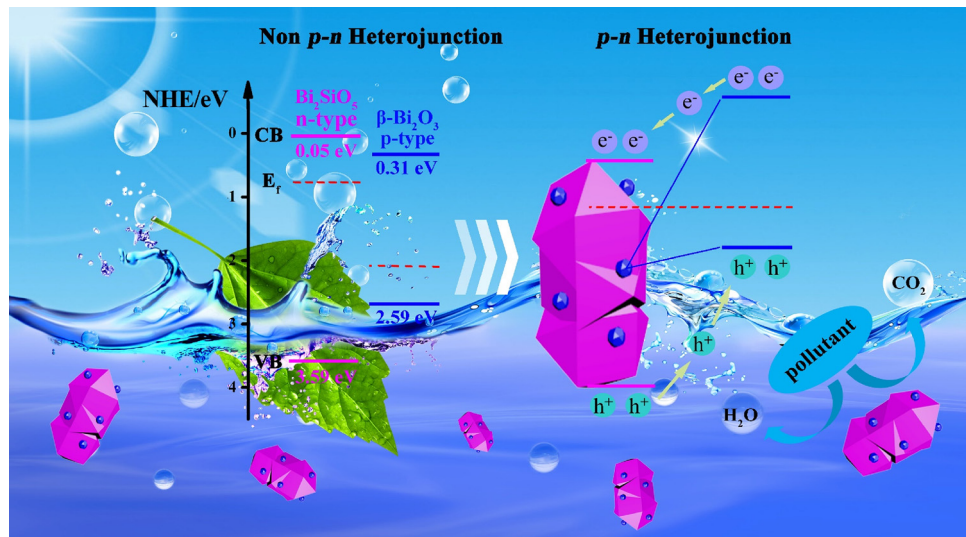


Fig. 8. The water contact angles of α -Bi₂O₃ (a) and BiSi-4 (b).

Scheme 1. The transformation from α - Bi_2O_3 to the β - Bi_2O_3 .Scheme 2. Schematic diagram of the proposed mechanism for the degradation of organic pollutants over the $\text{Bi}_2\text{O}_3/\text{Bi}_2\text{SiO}_5$ heterojunction photocatalysts under simulated solar light irradiation.

temperature, Bi_2SiO_5 was formed and it gradually coated on the surface of $\text{Bi}(\text{NO}_3)_3$. The Bi_2SiO_5 hindered the heat release of $\text{Bi}(\text{NO}_3)_3$ and the high-temperature metastable phase β - Bi_2O_3 were gradually produced [42]. As shown in Scheme 1, the crystal structure of α - Bi_2O_3 and β - Bi_2O_3 could be divided into different layers. The Bi layers of α - Bi_2O_3 and β - Bi_2O_3 are similar to each other, while the O layers of the α - Bi_2O_3 and β - Bi_2O_3 are greatly distorted, which are shown in Scheme 1 with solid black lines [43]. The alternating layers of Bi and O atoms are parallel to the y - z plane in α - Bi_2O_3 [44]. The Bi and O layers of β - Bi_2O_3 are parallel to the x - y plane. In addition, the O layers are more ordered in the x - y plane, while they are more dispersed along vertical direction than that of α - Bi_2O_3 . When Bi_2SiO_5 hindered the heat release of $\text{Bi}(\text{NO}_3)_3$, the O layers changed and β - Bi_2O_3 was formed.

Herein, a possible mechanism of $\text{Bi}_2\text{O}_3/\text{Bi}_2\text{SiO}_5$ heterojunction photocatalysts was proposed. The valence band positions of α - Bi_2O_3 , Bi_2SiO_5 and β - Bi_2O_3 are estimated to be 3.13, 3.59 and 2.59 eV, respectively. And the conduction band positions of α - Bi_2O_3 , Bi_2SiO_5 and β - Bi_2O_3 are estimated to be 0.33, 0.05 and 0.31 eV [26,45,46]. However, when p-type β - Bi_2O_3 and n-type Bi_2SiO_5 contacted with each other, a p-n heterojunction was formed at the interface of the phase

[47]. Moreover, the charge carriers at the two semiconductor interfaces were redistributed to balance the Fermi energy (E_f) and the Fermi levels of the two semiconductors tend to be consistent under equilibrium conditions [48]. Then, the band bending occurred in the space charge region, leading to the change of the internal electric field [49]. At the same time, both the location of CB and VB also changed at the Fermi level. When the Fermi level was consistent, the band positions of β - Bi_2O_3 moved up to the negative potential, while those of Bi_2SiO_5 moved in the opposite direction (As shown in Scheme 2) [48]. Under solar light irradiation, the electrons on the VB were excited and transfer to their CB, respectively, where they can react with O_2 and generate $\text{O}_2^{\cdot-}$. $\text{O}_2^{\cdot-}$ is a kind of reactive species and has strong oxidation ability. What is more, the excited electrons on the CB of β - Bi_2O_3 can transfer to the CB of Bi_2SiO_5 and the holes transfer in the opposite direction, which made that the separation of electron-hole pairs more effective and reduced the recombination of electron-hole pairs, enhancing the photocatalytic efficiency.

4. Conclusion

In this work, $\text{Bi}_2\text{O}_3/\text{Bi}_2\text{SiO}_5$ heterojunction photocatalysts were prepared by a facile one-step calcination method. The $\text{Bi}_2\text{O}_3/\text{Bi}_2\text{SiO}_5$ heterojunction photocatalysts exhibited much higher photocatalytic activity than $\alpha\text{-Bi}_2\text{O}_3$ on the degradation of organic pollutants under simulated sunlight irradiation. The enhanced photocatalytic activity could be ascribed to the larger specific surface area, the larger contact angle, the formation of $\beta\text{-Bi}_2\text{O}_3$ and construction of p-n heterojunction. More importantly, the phase transition mechanism of Bi_2O_3 in $\text{Bi}_2\text{O}_3/\text{Bi}_2\text{SiO}_5$ heterojunction photocatalyst was proposed, which is significant for the theoretical study and application of photocatalytic materials.

Acknowledgements

This work is supported by the National Natural Science Foundation of China (Grant No. 21577132 and 21777080), the Fundamental Research Funds for the Central Universities (Grant No. 2652015225) and the Students Innovation and Entrepreneurship Training Program 2017 (201711415025) of China University of Geosciences Beijing.

Appendix A. Supplementary data

Supplementary material related to this article can be found, in the online version, at doi:<https://doi.org/10.1016/j.apcatb.2018.05.069>.

References

- [1] Y. Fan, W. Ma, D. Han, S. Gan, X. Dong, L. Niu, *Adv. Mater.* 27 (2015) 3767–3773.
- [2] Z. Jiang, C. Zhu, W. Wan, K. Qian, J. Xie, *J. Mater. Chem. A* 4 (2016) 1806–1818.
- [3] C. Yu, G. Li, S. Kumar, K. Yang, R. Jin, *Adv. Mater.* 26 (2014) 892–898.
- [4] J. Guayaquil-Sosa, B. Serrano-Rosales, P. Valadés-Pelayo, H. de Lasa, *Appl. Catal. B Environ.* 211 (2017) 337–348.
- [5] Q. Hao, X. Niu, C. Nie, S. Hao, W. Zou, J. Ge, D. Chen, W. Yao, *Phys. Chem. Chem. Phys.* 18 (2016) 31410–31418.
- [6] Y. Jia, S. Zhan, S. Ma, Q. Zhou, *ACS Appl. Mater. Interface* 8 (2016) 6841–6851.
- [7] H. Mou, C. Song, Y. Zhou, B. Zhang, D. Wang, *Appl. Catal. B Environ.* 221 (2018) 565–573.
- [8] Y. Yu, C. Cao, H. Liu, P. Li, F. Wei, Y. Jiang, W. Song, *J. Mater. Chem. A* 2 (2014) 1677–1681.
- [9] Z. Mao, J. Chen, Y. Yang, D. Wang, L. Bie, B.D. Fahlman, *ACS Appl. Mater. Interface* 9 (2017) 12427–12435.
- [10] X. Pan, M. Yang, Y. Xu, *Phys. Chem. Chem. Phys.* 16 (2014) 5589–5599.
- [11] K. Wang, Q. Li, B. Liu, B. Cheng, W. Ho, J. Yu, *Appl. Catal. B Environ.* 176 (2015) 44–52.
- [12] C. Yu, F. Cao, G. Li, R. Wei, C.Y. Jimmy, R. Jin, Q. Fan, C. Wang, *Sep. Purif. Technol.* 120 (2013) 110–122.
- [13] K. Li, Z. Huang, X. Zeng, B. Huang, S. Gao, J. Lu, *ACS Appl. Mater. Interface* 9 (2017) 11577–11586.
- [14] Y. Bessekhouad, D. Robert, J. Weber, *J. Photochem. Photobiol. A* 163 (2004) 569–580.
- [15] P. Ju, P. Wang, B. Li, H. Fan, S. Ai, D. Zhang, Y. Wang, *Chem. Eng. J.* 236 (2014) 430–437.
- [16] F. Chen, Q. Yang, J. Sun, F. Yao, S. Wang, Y. Wang, X. Wang, X. Li, C. Niu, D. Wang, G. Zeng, *ACS Appl. Mater. Interface* 8 (2016) 32887–32900.
- [17] J. Park, B.G. Kim, S. Mori, T. Oguchi, *J. Solid State Chem.* 235 (2016) 68–75.
- [18] D. Liu, W. Yao, J. Wang, Y. Liu, M. Zhang, Y. Zhu, *Appl. Catal. B Environ.* 172 (2015) 100–107.
- [19] Y. Wu, M. Li, J. Yuan, X. Wang, *J. Mater. Sci.* (2017) 1–5.
- [20] Y. Kim, J. Kim, A. Fujiwara, H. Taniguchi, S. Kim, H. Tanaka, K. Sugimoto, K. Kato, M. Itoh, H. Hosono, *IUCrJ* 1 (2014) 160–164.
- [21] D. Liu, J. Wang, M. Zhang, Y. Liu, Y. Zhu, *Nanoscale* 6 (2014) 15222–15227.
- [22] L. Zhang, W. Wang, S. Sun, J. Xu, M. Shang, J. Ren, *Appl. Catal. B Environ.* 100 (2010) 97–101.
- [23] R. Chen, J. Bi, L. Wu, W. Wang, Z. Li, X. Fu, *Inorg. Chem.* 48 (2009) 9072–9076.
- [24] Z. Wan, G. Zhang, *J. Mater. Chem. A* 3 (2015) 16737–16745.
- [25] C. Yang, W.W. Lee, H. Lin, Y. Dai, H. Chi, C. Chen, *RSC Adv.* 6 (2016) 40664–40675.
- [26] Z. Bian, J. Zhu, S. Wang, Y. Cao, X. Qian, H. Li, *J. Phys. Chem. C* 112 (2008) 6258–6262.
- [27] A. Hameed, T. Montini, V. Gombac, P. Fornasiero, *J. Am. Chem. Soc.* 130 (2008) 9658–9659.
- [28] L. Zhang, W. Wang, S. Sun, D. Jiang, E. Gao, *CrystEngComm* 15 (2013) 10043–10048.
- [29] Q. Hao, R. Wang, H. Lu, W. Ao, D. Chen, C. Ma, W. Yao, Y. Zhu, *Appl. Catal. B Environ.* 219 (2017) 63–72.
- [30] X. Dai, Y. Luo, S. Fu, W. Chen, Y. Lu, *Solid State Sci.* 12 (2010) 637–642.
- [31] Y. Pang, X. Chen, C. Xu, Y. Lei, K. Wei, *Chemcatchem* 6 (2014) 876–884.
- [32] Q. Hao, S. Hao, X. Niu, X. Li, D. Chen, H. Ding, *Chin. J. Catal.* 38 (2017) 278–286.
- [33] T. Xie, Y. Liu, H. Wang, Z. Wu, *Appl. Surf. Sci.* 444 (2018) 320–329.
- [34] J. Zhang, Y. Lu, L. Ge, C. Han, Y. Li, Y. Gao, S. Li, H. Xu, *Appl. Catal. B Environ.* 204 (2017) 385–393.
- [35] J. Di, J. Xia, Y. Huang, M. Ji, W. Fan, Z. Chen, H. Li, *Chem. Eng. J.* 302 (2016) 334–343.
- [36] R. Hu, X. Xiao, S. Tu, X. Zuo, J. Nan, *Appl. Catal. B Environ.* 163 (2015) 510–519.
- [37] H. Song, R. Wu, J. Yang, J. Dong, G. Ji, *J. Colloid Interface Sci.* 512 (2018) 325–334.
- [38] J. Zeng, J. Zhong, J. Li, S. Huang, *Synth. React. Inorg. Met.* 45 (2015) 476–481.
- [39] X. Wang, Q. Wang, F. Li, W. Yang, Y. Zhao, Y. Hao, S. Liu, *Chem. Eng. J.* 234 (2013) 361–371.
- [40] X. Dang, X. Zhang, Y. Chen, X. Dong, G. Wang, C. Ma, X. Zhang, H. Ma, M. Xue, J. *Nanopart. Res.* 17 (2015) 93.
- [41] L. Shan, Y. Liu, C. Ma, L. Dong, L. Liu, Z. Wu, *Eur. J. Inorg. Chem.* (2016) 232–239.
- [42] T. Batu, J. Liu, Z. Cao, Y. Gao, W. He, C. Li, *Solid Waste Treat. Dispos.* 32 (2014) 81–85 In Chinese.
- [43] H. Deng, W. Hao, H. Xu, *Chinese Phys. Lett.* 28 (2011) 056101.
- [44] H. Harwig, J. Weenk, Z. Anorg. Allg. Chem. 444 (1978) 167–177.
- [45] S. Wu, J. Fang, W. Xu, C. Cen, J. Chem. Technol. Biotechnol. 88 (2013) 1828–1835.
- [46] L. Yang, S. Luo, Y. Li, Y. Xiao, Q. Kang, Q. Cai, *Chin. J. Catal.* 44 (2010) 7641–7646.
- [47] S. Han, J. Li, K. Yang, J. Lin, *Environ. Sci. Technol.* 36 (2015) 2119–2126.
- [48] J. Sun, X. Li, Q. Zhao, M.O. Tadé, S. Liu, *Appl. Catal. B Environ.* 219 (2017) 259–268.
- [49] D. Hou, X. Hu, P. Hu, W. Zhang, M. Zhang, Y. Huang, *Nanoscale* 5 (2013) 9764–9772.